 CMES, vol.91, no.5, pp.337-354, 2013

Iterative coupling between the TBEM and the MFS Part II - Elastic wave propagation

Julieta António[1], **António Tadeu**[1,2] **and Patrícia Ferreira**[3]

Abstract: The first of these two companion papers addressed the iterative coupling between a formulation based on the normal derivative of the integral equation (TBEM) and the method of fundamental solutions (MFS), which was used to solve scattering problems involving the propagation of acoustic waves in the vicinity of multiple thin barriers and domes. This second part extends these results to the more complicated case of in-plane wave propagation and presents their application to scattering problems involving SV-P waves. The formulation is first presented and verified by computing the number of iterations required and measuring the CPU time. Afterwards the formulation is used to simulate the propagation of waves generated by a blast load in the vicinity of a cavity driven in a cracked medium.

Keywords: elastic wave propagation, TBEM/MFS iterative coupling, cracked medium.

1 Introduction

The first of these two companion papers [Tadeu et al. (2013)] presented an iterative coupling between a formulation based on the normal derivative of the integral equation (TBEM) and the method of fundamental solutions (MFS) to solve the propagation of acoustic waves in the vicinity of multiple thin barriers and domes. This second part extends this method to the more complicated case of elastic wave propagation.

The applicability of the proposed formulation is illustrated by solving physical systems, involving varying numbers of inclusions (cracks), and the CPU time taken is compared with the times needed for a full coupling technique.

[1] CICC, Department of Civil Engineering, Faculty of Sciences and Technology, University of Coimbra, Rua Luís Reis Santos - Pólo II da Universidade, 3030-788 Coimbra, Portugal

[2] Corresponding author. E-mail address: tadeu@itecons.uc.pt Tel. + 351 239 798 921 Fax: + 351 239 798 939

[3] ITeCons, Rua Pedro Hispano, Pólo II da Universidade, 3030-289 Coimbra, Portugal

The next section sets out the iterative coupling formulation applied to multiple cracks and cavities embedded in an unbounded elastic medium. The TBEM is used to model empty cracks while the MFS simulates the cavities. The performance of the iterative coupling formulation is verified against solutions obtained using a full TBEM/MFS coupling formulation, which are used as reference solutions.

The number of iterations and the CPU time taken to compute the numerical responses when varying numbers of inclusions are subjected to different steady state line blast sources are used to evaluate the computational efficiency of the proposed iterative coupling formulation.

Finally, the applicability of the proposed iterative method is shown by means of a numerical example that simulates the propagation of elastic waves generated by a line source when a set of circular empty cracks are embedded in the vicinity of an empty circular cavity in an unbounded elastic medium. Time signatures are computed to illustrate the main propagation features.

2 Iterative TBEM/MFS coupling formulation

The iterative process follows the procedure used for the acoustic problem [Tadeu et al. (2013)]. At each iteration step, each inclusion is solved individually, assuming there are no other inclusions present. The incident field is the scattered field generated by all the other previously solved inclusions. At the first iteration, the direct incident field generated by the source and exciting the field, needs also to taken into account. This procedure is briefly described next, using two inclusions.

Consider two empty irregular two-dimensional cylindrical inclusions, a crack and a cavity, embedded in a homogeneous elastic medium (Medium 1) with density ρ (Figure 1) and allowing longitudinal (P-wave) and shear waves (S-wave) to travel at velocities α and β, respectively.

It is further assumed that this system is subjected to a dilatational line source placed at x_s, $(x_s,\ y_s)$. The incident wave field generated by this source can be expressed in the frequency domain, ω, by means of the classic dilatational potential:

$$\varphi_{inc}(x,\omega) = -A\mathrm{H}_0(k_\alpha r_1) \tag{1}$$

Thus, the displacement field in direction i, at x, $(x,\ y)$, can be expressed as

$$u_{i\_inc}(x,x_s,\omega) = Ak_\alpha \mathrm{H}_1(k_\alpha r_1)\frac{\partial r_1}{\partial x_i} \tag{2}$$

where the subscript *inc* represents the incident field, $r_1 = \sqrt{(x-x_s)^2+(y-y_s)^2}$, A the wave amplitude, $k_\alpha = \frac{\omega}{\alpha}$ and $H_n(\ldots)$ correspond to second Hankel functions of order n.

Iteration 0 - Step 1: The incident field only illuminates the crack, and the second inclusion is assumed to be absent (see Figure 2a)

The displacement field in an infinite, homogeneous and isotropic elastic medium is governed, in the frequency domain, by the expression,

$$(\lambda + 2\mu)\nabla(\nabla \bullet u) - \mu\nabla \times (\nabla \times u) = -\omega^2 \rho u \tag{3}$$

where u represents the displacement vector, and λ and μ are the Lamé constants.

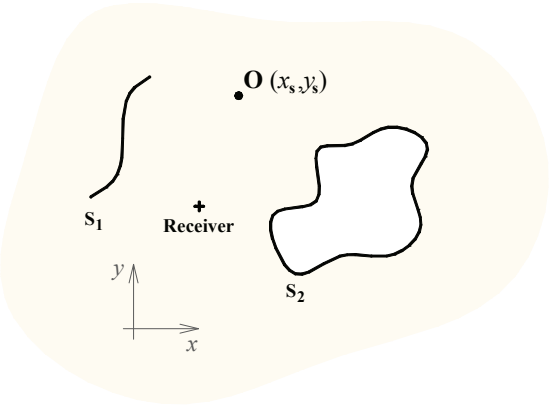

Figure 1: The geometry of the problem

The boundary element method (BEM) formulation fails when modeling the scattered wave field in the vicinity of thin empty inclusions, such as cracks. The traction boundary element method (TBEM) is often proposed to get over that difficulty [2,3]. This formulation can be expressed by the following equation:

$$a u_i^{(0)}(x_0, \omega) = -\int_{S_1} u_j^{(0)}(x, \omega)\, \overline{H}_{ij}(x, n_{n1}, n_{n2}, x_0, \omega)\, \mathrm{d}s + \overline{u}_{i\_inc}(x_0, n_{n2}, x_s, \omega) \tag{4}$$

This equation can be seen as resulting from the application of dipoles (dynamic doublets). In this equation, i, $j = 1, 2$ correspond to the normal and tangential directions relative to the inclusion surface. In these equations, n_{n2} is the unit outward normal to the boundary S_1 at the collocation points x_0, (x_0, y_0), whilen_{n1} is the unit outward normal along boundary S_1, at x, defined by the vector $n_{n1} = (\cos\ \theta_{n1},\ \sin\ \theta_{n1})$. The Green's functions $\bar{H}_{ij}(x, n_{n1}, n_{n2}, x_0, \omega)$ are defined by applying the traction operator to $H_{ij}(x, n_{n1}, x_0, \omega)$, which can be obtained by combining the derivatives of the former Green's functions, in order to x and y, so as

to obtain stresses [Amado Mendes and Tadeu (2006)]. $H_{ij}(x,n_{n1},x_0,\omega)$ define the fundamental solutions for tractions (Green's functions [Tadeu and Kausel (2000)]), in direction j on the boundary S_1 at x, caused by a unit point force in direction i applied at the collocation point, x_0. $u_j^{(0)}(x,\omega)$ corresponds to displacements in direction j at x. The superscript used in $u_j^{(iter)}$ indicates the number of the iteration. The incident field, $\overline{u}_{i\_inc}(x_0,n_{n2},x_s,\omega)$, can be evaluated in a similar way to the evaluation of $\bar{H}_{ij}$, in terms of stresses. As noted by Guiggiani (1998) the coefficient a is zero for piecewise straight boundary elements.

The boundary integral equation (4) can be solved by discretizing the boundary into straight boundary elements, with one nodal point in the middle of each element. A set of integrations therefore needs to be calculated, and this is done by applying a Gaussian quadrature scheme to elements that are not the loaded elements. If the elements happen to be the loaded ones, hyper-singular integrals arise and they are evaluated. These hyper-singular integrals are evaluated by means of an indirect approach that represents the dynamic equilibrium of a semi-cylinder, detached immediately above the boundary element [Amado Mendes and Tadeu (2006)].

The use of N boundary elements leads to a system of $[2N \times 2N]$ equations ($\underline{\underline{B}}\underline{u}^{(0)} = \underline{u}_{inc}^{(0)}$),

$$\left[-\bar{H}_{ij}^{kl}\right]\left[u_j^{(0)l}\right] = \left[-u_{i\_inc}^{(0)k}\right] \tag{5}$$

where $k,l = 1,N$, $\bar{H}_{ij}^{kl} = \int_{C_l} \overline{H}_{ij}(x_l,n_{n1},n_{n2},x_k,\omega)\,dC_l$, C_l is the length of each boundary element and $u_{i\_inc}^{(0)k} = \overline{u}_{i\_inc}(x_k,n_{n2},x_s,\omega)$.

The solution of this system of equations gives the nodal displacements $u_j^{(0)}$ along the boundary S_1, which allows the scattered displacement field to be defined at any receiver x_{rec},

$$u_{i,01}(x_{rec},\omega) = -\int_{S_1} u_j^{(0)}(x,\omega)\; H_{ij}(x,n_{n1},n_{n2},x_{rec},\omega)\;\mathrm{d}s \tag{6}$$

In this equation, the subscripts 01 in $u_{i,01}^{(0)}(x_{rec},\omega)$ define the iteration order (0) and identify the inclusion structure that produces it (1).

Iteration 0 - Step 2: The cavity is subjected to the direct incident field and illuminated by the scattered field generated at the crack after being submitted to the incident field (step 1) (see Figure 3a).

The cavity is modeled using the MFS. The MFS assumes that the response of this neighbouring inclusion is found as a linear combination of fundamental solutions

simulating the displacement field generated by NS virtual sources. These virtual loads are distributed along the inclusion interface S_2 at a distance δ from that boundary, towards the interior (line $\hat{C}^{(1)}$ in Fig. 3b), in order to prevent singularities. Sources inside the inclusion have unknown amplitudes $a_{nj,n\_ext}^{(iter)}$ (the superscript $(iter)$ indicates the number of the iteration). In the exterior elastic medium the scattered displacement fields are given by:

$$u_i^{(0)}(x,\omega) = \sum_{n=1}^{NS} \sum_{j=1}^{2} \left[a_{nj,n\_ext}^{(0)} G_{ji}(x, x_{n\_ext}, \omega) \right] \tag{7}$$

where $G_{ji}(x, x_{n\_ext}, \omega)$ are the fundamental solutions which represent the displacements at points x in the medium, in direction i, caused by a unit point force in direction j applied at positions x_{n_ext}. n_ext are the subscripts that denote the load order number placed along line $\hat{C}^{(1)}$.

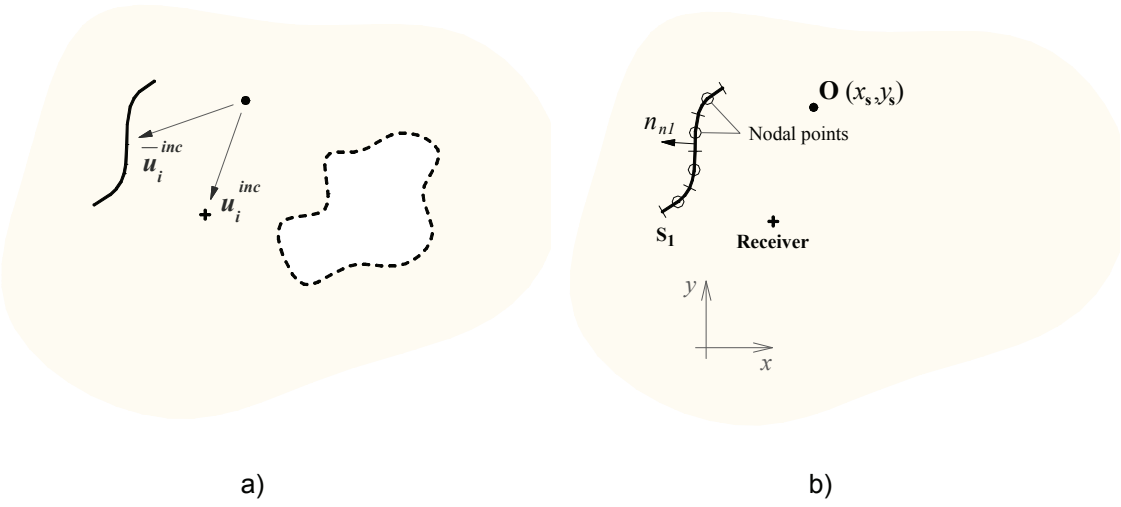

Figure 2: Iteration 0, step 1: a) geometry of the problem; b) discretization of the crack: nodal points and boundary elements

The amplitudes of the unknown virtual loads $a_{nj,n\_ext}^{(iter)}$ can only be evaluated if null tractions are imposed along the boundary S_2 along the NS collocation points x_{col}. This must be done taking into account the scattered field generated at inclusion 1, the crack, which can be viewed as an incident field that strikes the second inclusion $\overline{u}_{i,12}^{(0)}(x_{col}, n_{n2}, \omega) = -\int_{S_1} u_j^{(0)}(x,\omega)\, \overline{H}_{ij}(x, n_{n1}, n_{n2}, x_{col}, \omega)\, \mathrm{d}s$. So Eq. (7) needs to

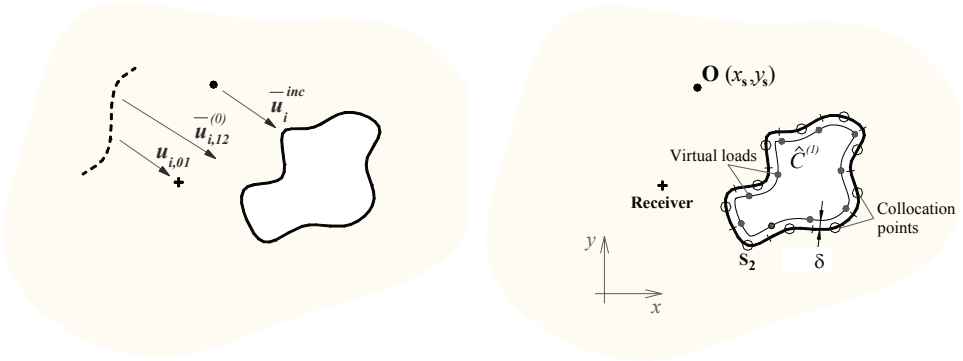

Figure 3: Iteration 0, step 2: a) geometry of the problem; b) cavity: nodal points and boundary elements

be modified accordingly,

$$\overline{u}_{i,12}^{(0)}(x_{col}, n_{n2}, \omega) + \overline{u}_{i\_inc}(x_{col}, n_{n2}, x_s, \omega) + \sum_{n=1}^{NS}\sum_{j=1}^{2}\left[a_{nj,n\_ext}^{(0)}\overline{G}_{ji}(x_{col}, n_{n2}, x_{n\_ext}, \omega)\right] = 0 \quad (8)$$

The Green's functions $\overline{G}_{ji}(x_{col}, n_{n2}, x_{n\_ext}, \omega)$ are defined by applying the traction operator to $G_{ij}^{(1)}(x, y, x_{col}, y_{col}, \omega)$, which can be obtained by combining the derivatives of the former Green's functions, in order to x and y, so as to obtain the stresses [Castro and Tadeu (2012)]. In these equations, n_{n2} is the unit outward normal to the boundary S_2 at the collocation points x_{col}.

This leads to a system of $[2NS \times 2NS]$ equations ($\underline{\underline{C}}a^{(0)} = \underline{\overline{u}}_{inc}^{(0)}$), which allows the unknown amplitudes$a_{nj,n_ext}^{(0)}$ to be defined.

$$\left[-\overline{G}_{ji}^{nn}\right]\left[a_{nj,n\_ext}^{(0)}\right] = \left[-u_{i\_inc}^{(0)}\right] \quad (9)$$

where $n = 1, NS$, $u_{i\_inc}^{(0)} = \overline{u}_{i,12}^{(0)}(x_{col}, n_{n2}, \omega) + \overline{u}_{i\_inc}(x_{col}, n_{n2}, x_s, \omega)$.
The scattered field at x_{rec} can be computed as

$$u_{i,02}(x_{rec}, \omega) = \sum_{n=1}^{NS}\sum_{j=1}^{2}\left[a_{nj,n\_ext}^{(0)}G_{ji}(x_{rec}, x_{n\_ext}, \omega)\right] \quad (10)$$

At the end of this iteration the total displacement field at the receiver would be

$$u_i(x_{rec},\omega) = u_{i\_inc}(x_{rec},x_s,\omega) + \sum_{m=1}^{M} u_{i,0m}(x_{rec},\omega) \tag{11}$$

In this case $M = 2$ (the number of inclusions).

Iteration k - Step 1: The first inclusion is only illuminated by the field scattered by the second inclusion in the conditions defined in the iteration k-1 at Step 2 (see Figure 4a).

The incident field is the scattered field generated in the previous iteration by the second inclusion

$$\overline{u}_{i,21}^{(k-1)}(x_0,n_{n2},x_{n\_ext},\omega) = \sum_{n=1}^{NS}\sum_{j=1}^{2}\left[a_{nj,n\_ext}^{(k-1)}\overline{G}_{ji}(x_0,n_{n2},x_{n\_ext},\omega)\right] \tag{12}$$

which leads to

$$a\,u_i^{(k)}(x_0,\omega) = -\int_{S_1} u_j^{(k)}(x,\omega)\ \overline{H}_{ij}(x,n_{n1},n_{n2},x_0,\omega)\ \mathrm{d}s + \overline{u}_{i,21}^{(k-1)}(x_0,n_{n2},x_{n\_ext},\omega) \tag{13}$$

A system of $[2N \times 2N]$ equations similar to the previous one at iteration 0 is required to solve Eq. (13), where only the constant matrix needs to be modified ($\underline{\underline{B}}\underline{u}^{(k)} = \underline{u}_{inc}^{(k)}$). Thus, if during iteration 0 the system has been solved by defining its inverse matrix $\underline{\underline{B}}^{-1}$, the new solution does not require the system to be solved, $\underline{u}^{(k)} = \underline{\underline{B}}^{-1}\underline{u}_{inc}^{(k)}$.

The scattered pressure field at the receiver x_{rec} can then be calculated as

$$u_{i,k1}(x_{rec},\omega) = -\int_{S_1} u_j^{(k)}(x,\omega)\ H_{ij}(x,n_{n1},n_{n2},x_{rec},\omega)\ \mathrm{d}s \tag{14}$$

Iteration k - Step 2: The second inclusion is now only illuminated by the field scattered by the first inclusion at Step 1 (see Figure 4b).

The stress field generated by the first inclusion at *Step 1* is the only incident field that strikes the cavity $\overline{u}_{i,12}^{(k)}(x_{col},n_{n2},\omega) = -\int_{S_1} u_j^{(k)}(x,\omega)\ \overline{H}_{ij}(x,n_{n1},n_{n2},x_{col},\omega)\ \mathrm{d}s$,

which leads to

$$\overline{u}_{i,12}^{(k)}(x_{col},n_{n2},\omega) + \sum_{n=1}^{NS}\sum_{j=1}^{2}\left[a_{nj,n\_ext}^{(k)}\overline{G}_{ji}(x_{col},n_{n2},x_{n\_ext},\omega)\right] = 0 \tag{15}$$

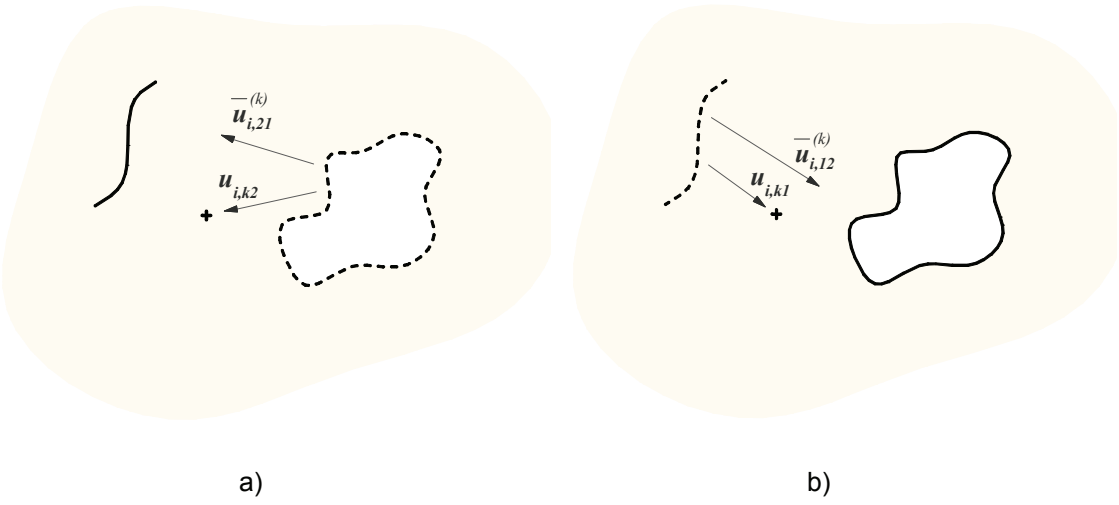

Figure 4: Iteration k: a) step 1; b) step 2

This leads to the system of $[2NS \times 2NS]$ equations ($\underline{\underline{C}} a^{(k)} = \underline{\overline{u}}^{(k)}_{inc}$), similar to the one defined before in equation (9) where only the constant matrix needs to be replaced by $u^{(k)}_{i\_inc} = \overline{u}^{(k)}_{i,12}(x_{col}, n_{n2}, \omega)$. The values $a^{(k)}_{nj,n\_ext}$ can thus be obtained as $\underline{a}^{(k)} = \underline{\underline{C}}^{-1} \underline{\overline{u}}^{(k)}_{inc}$.

The new scattered field produced by this inclusion at x_{rec} is then

$$u_{i,k2}(x_{rec}, \omega) = \sum_{n=1}^{NS} \sum_{j=1}^{2} \left[a^{(k)}_{nj,n\_ext} G_{ji}(x_{rec}, x_{n\_ext}, \omega) \right] \tag{16}$$

At the end of iteration k the total displacement field at the receiver would be

$$u_i(x_{rec}, \omega) = u_{i\_inc}(x_{rec}, x_s, \omega) + \sum_{iter=0}^{k} \sum_{m=1}^{M} u_{i,iter\,m}(x_{rec}, \omega) \tag{17}$$

The iterative process continues until the contribution of the scattered field to the displacement at a certain receiver reaches a predefined threshold.

The proposed iterative coupling requires only the solution of the individual inclusions' linear system of equations. Given the example used to illustrate the algorithm procedure, the two individual systems of $[2N \times 2N]$ and $[2NS \times 2NS]$ equations would only need to be solved once. The full coupling would require solving a system of $[2(N+NS) \times 2(N+NS)]$ equations. This process would be more relevant if there were a large number of inclusions, when the size of the system of

equations used by the full coupling would be larger than the systems associated with each inclusion, as used in the proposed iterative coupling.

3 Performance of the proposed iterative coupling formulation

The performance of the proposed iterative coupling algorithm (MFS/TBEM) was checked by applying it to solve the elastic field produced by a steady state blast line load emitting different excitation frequencies and placed in the presence of circular empty cracks embedded in the vicinity of an empty cavity in an unbounded elastic medium.

The CPU time is computed and compared with the times obtained for a full coupling formulation.

The null-thickness, 90° arc-shaped cracks, are centered at $(5.0\,\mathrm{m},\ 20.0\,\mathrm{m})$, have radii of 6.00 m and each has a length of 3 π m. They are equally spaced when all three cracks are in place at the same time. The empty cavity is centered at $(20.0\,\mathrm{m},\ 9.0\,\mathrm{m})$ and has a radius of 4.0 m (see Fig. 5).

Three separate problems are solved by combining the number of the crack inclusions, viz. one crack inclusion (Case 1), two crack inclusions (Case 2) and three crack inclusions (Case 3).

Each crack is discretized as an open line and loaded with dipole loads (200 TBEM boundary elements), while the cavity boundary is modeled using 160 virtual sources placed at 0.8 m from the inclusion surface.

The host medium, with a density of 2200 kg/m^3, allows P-wave and S-wave velocities of 1651.4 m/s and 1011.3 m/s, respectively. This system is illuminated by a wave field generated by a dilatational line load placed within the subdomain defined by the three cracks, at $(0.0\,\mathrm{m},\ 20.0\,\mathrm{m})$.

The resulting displacement is obtained over a grid of 18268 receivers arranged along the x and y directions at equal intervals and placed from $x = -5.0$m to $x = 25.0$ m and from $y = -10.0$ m to $y = 30.0$ m.

For each case the real and imaginary parts of the x and $y-$displacement field obtained using the full coupling formulation are computed and the associated CPU time is registered at each receiver.

The number of iterations and the CPU time required at each receiver is also calculated with the proposed iterative coupling formulation. The definition of the number of iterations results from the imposition of a convergence criterion at each receiver, by which the difference between the displacement obtained at two succes-

sive iterations satisfies the following condition

$$\left| \sum_{iter=0}^{k} \sum_{m=1}^{M} u_{i,iter\,m}(x_{rec},\omega) - \sum_{iter=0}^{k-1} \sum_{m=1}^{M} u_{i,iter\,m}(x_{rec},\omega) \right| / \left| \sum_{iter=0}^{k} \sum_{m=1}^{M} u_{i,iter\,m}(x_{rec},\omega) \right| \leq 1E-05. \quad (18)$$

The computations have been performed for two excitation frequencies, $f = 4.0$ Hz and $f = 200.0$ Hz, with a small imaginary part of the form $\omega_c = \omega - i\eta$ (in which $\eta = 0.7\Delta\omega = 0.7\text{x}2\pi\text{x}4$). As can be seen in Figures 6 – 8, the number of iterations varies with the position of each receiver.

The number of iterations needed for each case is higher when the excitation frequency is higher.

The CPU time and the number of iterations increase the greater the number of cracks, as expected. In all cases the iterative coupling performs better than the full coupling. However, the iterative coupling seems to work better when the number of cracks to be modeled is higher.

Additional simulations have been performed using the same frequencies but with different imaginary parts (not illustrated). As in Part I it was found that as the frequency increment increases the number of iterations and CPU time decrease, while the opposite occurs for decreasing frequency increments. This is because a smaller $\Delta\omega$ is associated with a larger time window, which accounts for a larger number of multi-reflections.

4 Time responses using the proposed iterative coupling formulation

The usefulness of the proposed iterative coupling algorithm (TBEM/MFS) is illustrated by solving the elastic field produced by a blast line load placed in the presence of circular empty cracks embedded in the vicinity of an empty cavity in an unbounded elastic medium with the geometry described for Case 3. The properties assumed for the elastic medium are the same as described above.

Each crack is discretized as an open line using the TBEM and discretization uses a number of boundary elements that changes from frequency to frequency. A ratio of 8 between the wavelength and the length of the boundary element was used. In any case a minimum number of 80 boundary elements was set to model each crack. The cavity boundary is modeled by the MFS, using virtual loads/collocation points that changed from frequency to frequency according to the ratio between the wavelength and the distance between collocation points, which was set at 8. A minimum of 160 virtual loads/collocation points were used. In the present example, the virtual loads are placed 0.8 m from the cavity's boundary.

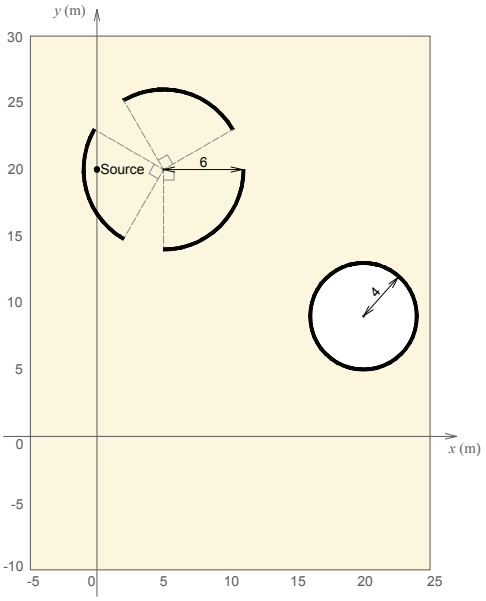

Figure 5: Geometry of the problem

This system is illuminated by a wave field generated by a dilatational line load placed in the subdomain defined by the three cracks, at $(0.0\,\mathrm{m},\ 20.0\,\mathrm{m})$, modeled as a Ricker wavelet with a characteristic frequency of 500Hz. The computations are performed in the frequency domain for frequencies ranging from 4.0 Hz to 2048.0 Hz, with a frequency increment of 4.0 Hz, which determines a total time window of 0.25 s.

The resulting displacement is obtained over a grid of receivers arranged as described before.

A set of snapshots taken from computer animations is presented in Fig. 9 to illustrate the resulting wave field at different time instants in terms of x- and y- displacement components (u_x and u_y). These displacement fields correspond to the incident field generated by the 2D source plus the scattered field generated by the thin cracks and empty inclusion.

The color scale adopted ranges from blue (lower displacement values) to red (higher displacement values).

The waves excited by the dilatational source first hit the surface of the crack that is furthest to the left. The waves are all reflected back as P- and S-waves, but they are as yet indistinguishable as they overlap. At $t = 1.83$ ms (see Figure 9a)

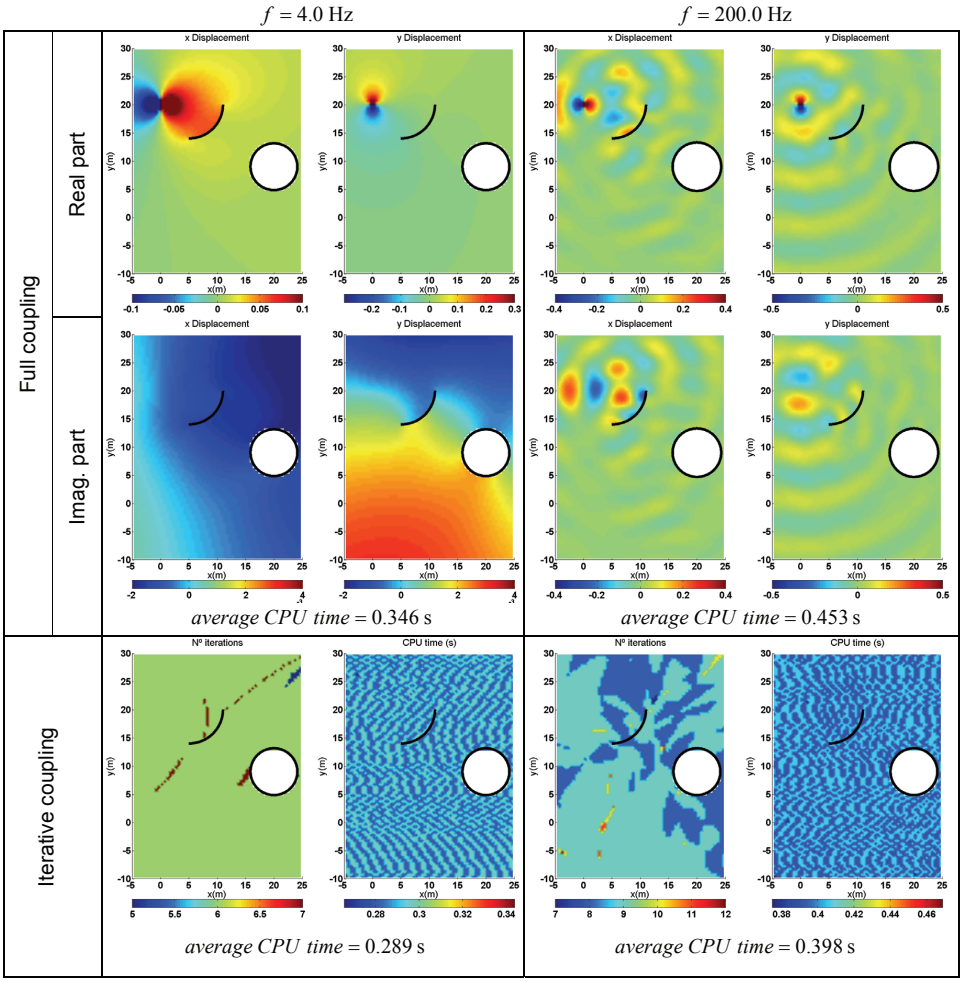

Figure 6: Elastic problem – one crack

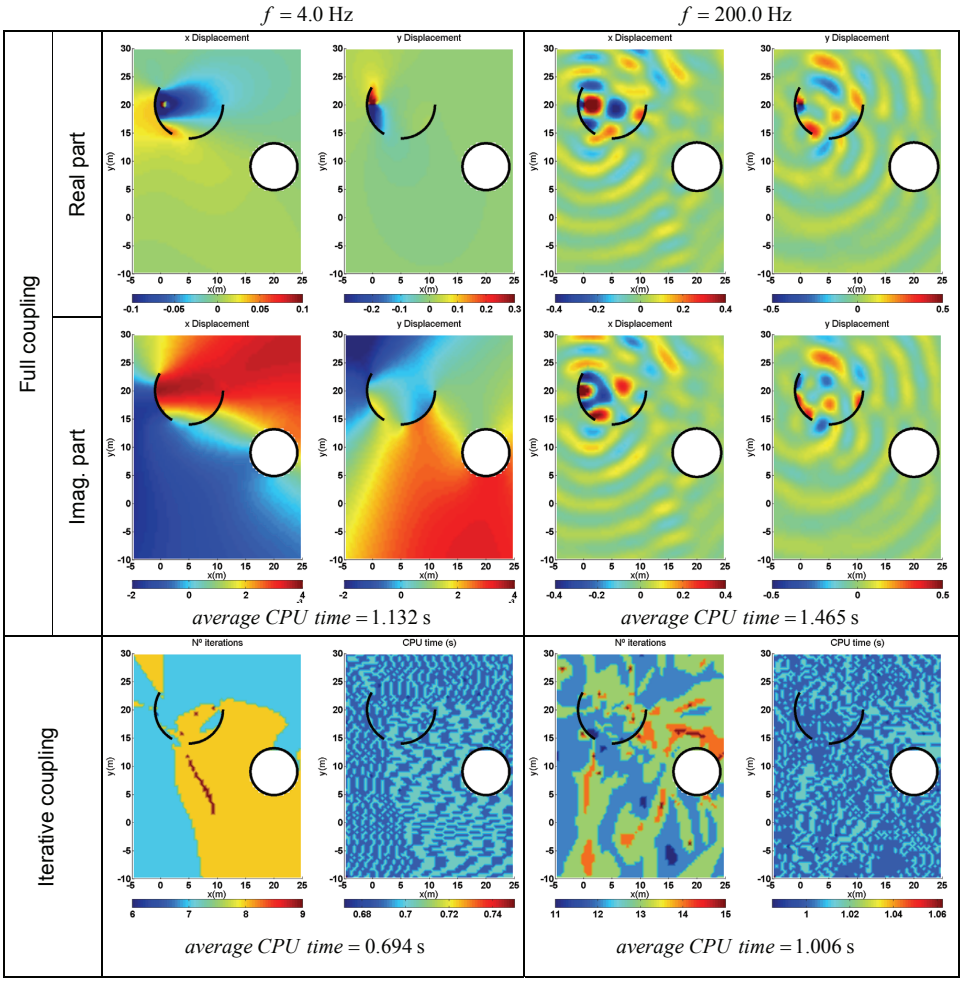

Figure 7: Elastic problem – two cracks

the diffracted wavefield is evident around the top of the crack. At $t = 5.49$ms the wavefront has reached the other two cracks. Additional diffractions can be seen at the edges of the cracks as well additional reflections at their surface (see Figure 9b). The wave front has reached the rightmost gap between the cracks.

The wave energy trapped within the subdomain defined by the concave part of the cracks generates a complex wave field due to the multiple reflections, whereas the energy diffracted at the edges of the cracks spreads out through the gaps between the cracks, propagates away and reaches the surface of the empty cavity, whence it is reflected back (see Figure 9c at $t = 13.12$ms). Very well-developed P- and S-waves can be observed propagating and travelling at different velocities through the unbounded elastic medium.

As time passes, the wavefield becomes more and more intricate due to the interaction of the different diffracted and reflected waves, as can be observed at $t = 24.41$ms in Figure 9d.

5 Conclusions

The TBEM and the MFS have been coupled using an iterative formulation to solve elastic scattering problems within a domain that incorporates cavities and cracks. The MFS was used to model the cavities, thus avoiding the discretization of the boundary and the need of integrals, as required by boundary element methods. The TBEM was used to model the cracks where the classical formulation of the boundary element method fails and the application of the MFS requires the domain decomposition. The iterative procedure allows the scattered field created by a large number of inclusions to be computed by using a series of systems of equations that are smaller than those required when a full coupling is applied.

The effectiveness of the proposed iterative coupling formulation was checked by computing the CPU time required and comparing it with that used by a full coupling formulation. The number of iterations has also been calculated with the iterative formulation. The CPU time and the number of iterations both increase for higher excitation frequencies and when the number of inclusions increases. In all cases the iterative coupling requires less CPU time than the full coupling. The iterative coupling has proven to be more advantageous when the number of cracks to be modeled is greater. The applicability of the proposed iterative formulation has been illustrated by computing the responses generated by the elastic wave propagation in the vicinity of a cavity and cracks.

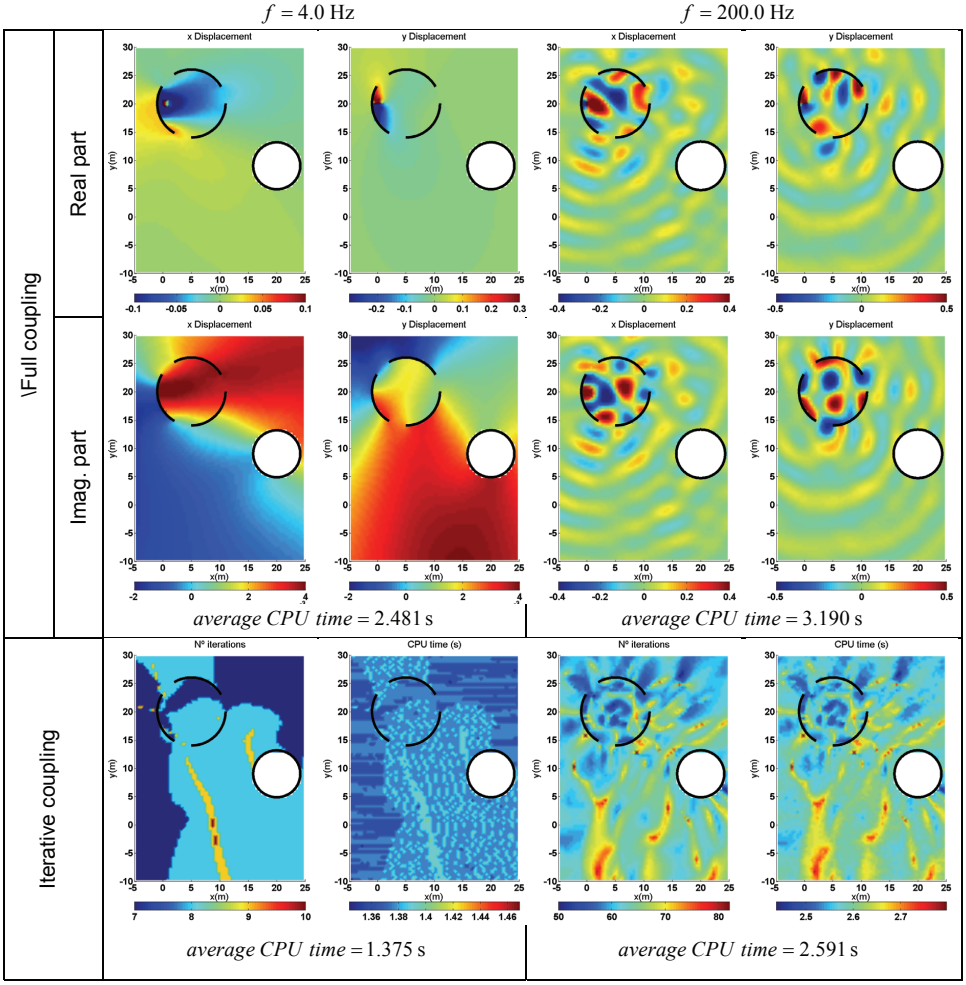

Figure 8: Elastic problem – three cracks

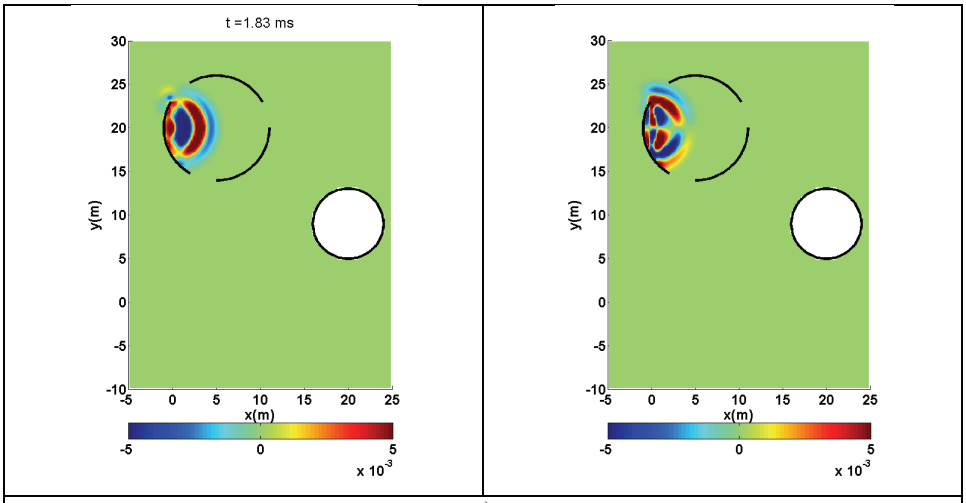

a)

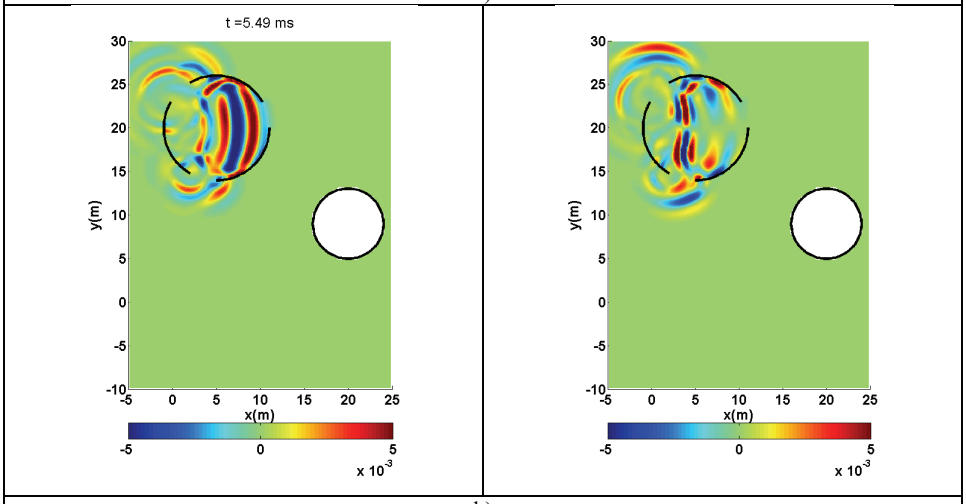

b)

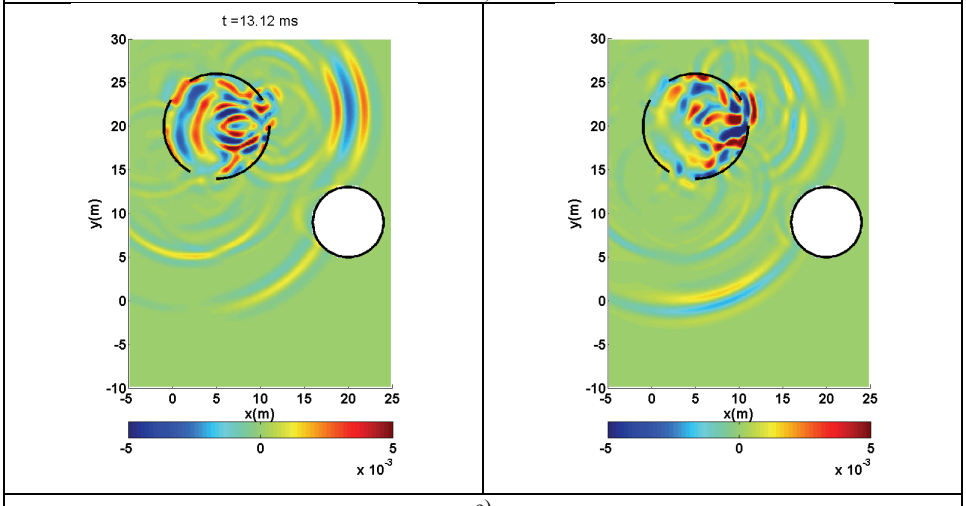

c)

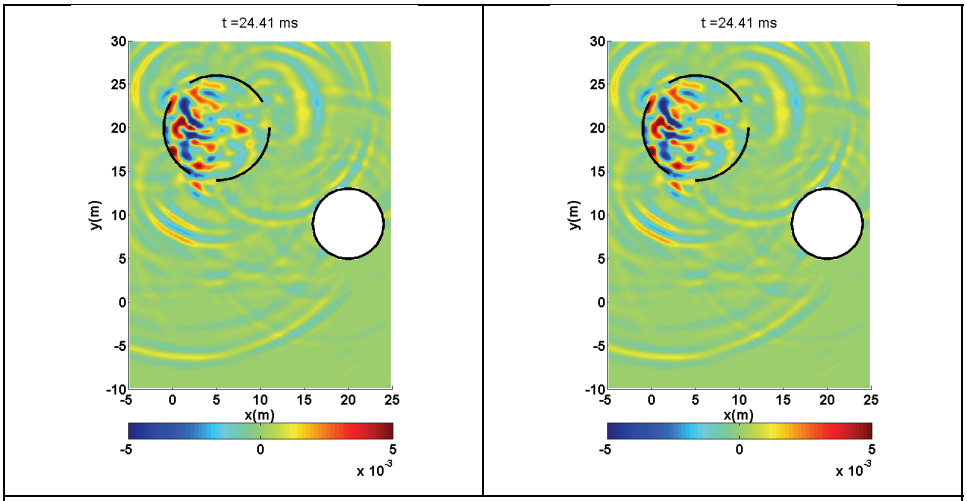

Figure 9: Time domain displacements u_x (left column) and u_y (right column) for Case 3 for a characteristic frequency of 500 Hz a) $t = 1.83$ ms; b) $t = 5.49$ms; c) $t = 13.12$ ms; d) $t = 24.41$ ms

References

Amado Mendes, P.; Tadeu, A. (2006): Wave propagation in the presence of empty cracks in an elastic medium. *Computational Mechanics*, vol. 38, no. 3,pp. 183-199.

Castro, I.; Tadeu, A. (2012): Coupling the BEM/TBEM and the MFS for the numerical simulation of elastic wave propagation *Engineering Analysis with Boundary Elements*, vol. 36, pp. 169-180.

Guiggiani M. (1998): Formulation and numerical treatment of boundary integral equations with hypersingular kernels. In: Sladek V, Sladek J, editors. *Singular Integrals in Boundary Element Methods*. Southampton and Boston: Comput. Mech. Publications.

Prosper D.; Kausel E. (2001): Wave scattering by cracks in laminated media. In: Atluri SN, Nishioka T, Kikuchi M (eds), *CD: Advances in Computational Engineering and Sciences*. Proceedings of the international Conference on Computational Engineering and Science ICES'01, Puerto Vallarta, Mexico,19-25/08/2001. Tech Science Press

Tadeu A.; Kausel E. (2000): Green's Functions for Two-and-a-half Dimensional Elastodynamic Problems. *J. Eng. Mech.* vol. 126, no. 10, pp. 1093-1097.

Tadeu, A.; António, J.; Ferreira, P. (2013): Iterative coupling between the BEM/TBEM and the MFS. Part I - Acoustic wave propagation. *Computer Modeling in Engineering & Sciences* vol.91, no. 3, pp.153–176.